

# **The intracellular pathway for MR1 presentation of vitamin B-related antigens**

Hamish E.G. McWilliam<sup>1,2,7</sup>, Sidonia B.G. Eckle<sup>1</sup>, Alex Theodossis<sup>2</sup>, Ligong Liu<sup>3,4</sup>, Zhenjun Chen<sup>1</sup>,  
Jacinta M. Wubben<sup>2,7</sup>, David P. Fairlie<sup>3,4</sup>, Richard A. Strugnell<sup>1</sup>, Justine D. Minter<sup>5</sup>, James  
McCluskey<sup>1</sup>\*, Jamie Rossjohn<sup>2,6,7</sup>\* and Jose A. Villadangos<sup>1,5</sup>\*

<sup>1</sup>Department of Microbiology and Immunology, Doherty Institute of Infection and Immunity, The University of Melbourne, Parkville, Victoria 3010, Australia.

<sup>2</sup>Infection and Immunity Program and The Department of Biochemistry and Molecular Biology, Biomedicine Discovery Institute Monash University, Clayton, Victoria 3800, Australia.

<sup>3</sup>Division of Chemistry & Structural Biology, Institute for Molecular Bioscience, The University of Queensland, Brisbane, Queensland 4072, Australia.

<sup>4</sup>ARC Centre of Excellence in Advanced Molecular Imaging, The University of Queensland, Brisbane, Queensland 4072, Australia.

<sup>5</sup>Department of Biochemistry and Molecular Biology, Bio21 Molecular Science and Biotechnology Institute, The University of Melbourne, Parkville, Victoria 3010, Australia.

<sup>6</sup>Institute of Infection and Immunity, Cardiff University School of Medicine, Heath Park, Cardiff CF14 4XN, UK.

<sup>7</sup>Australian Research Council Centre of Excellence in Advanced Molecular Imaging, Monash University, Clayton, Victoria 3800, Australia

\* Joint senior and corresponding authors James McCluskey, jamesm1@unimelb.edu.au; Jamie Rossjohn, jamie.rossjohn@monash.edu; and Jose A Villadangos, j.villadangos@unimelb.edu.au.

## **ABSTRACT**

**MR1 presents vitamin B-related antigens (“VitB Ags”) to Mucosal-Associated Invariant T (MAIT) cells using an uncharacterized pathway. We show that, unlike other antigen-presenting molecules, MR1 does not constitutively present self-ligands. In the steady-state it accumulates in a ligand-receptive conformation within the endoplasmic reticulum. VitB Ags reach this location and form a Schiff base with MR1, triggering a “molecular switch” that allows MR1-VitB Ag complexes to traffic to the plasma membrane. These complexes are endocytosed with kinetics independent of the affinity of the MR1-ligand interaction and degraded intracellularly, although some MR1 molecules acquire new ligands during passage through endosomes and recycle back to the surface. MR1 antigen presentation is characterized by a rapid “off-on-off” mechanism strictly dependent on antigen availability.**

## INTRODUCTION

The mechanisms that enable cells to present antigens (Ags) on their surface for inspection and recognition by T lymphocytes are central to the cellular arm of protective immunity. Ags can vary in chemical composition and origin and the capacity of distinct T cell populations to discern these different Ags underpins the ability of the immune system to mount effective responses against each specific challenge. Each T cell population is specialized at recognizing Ags bound to a particular type of Ag presenting molecule, namely Major Histocompatibility Complex class I (MHC I), MHC class II (MHC II) and MHC I-like molecules<sup>1</sup>. In turn, each Ag-presenting molecule is specialized in the acquisition of its antigenic cargo in different intracellular locations, assisted by a cohort of accessory proteins required for folding, trafficking, ligand processing and ligand binding.

MHC I molecules constitutively present peptides derived from polypeptides degraded in the cytosol, chiefly by the proteasome<sup>2</sup>. These peptides are transported into the ER by a dedicated TAP transporter, trimmed to optimal size by specialized proteases, and loaded into the peptide-binding site of newly synthesized MHC I molecules. The MHC I-peptide complexes then follow the secretory pathway to the plasma membrane, where they remain until the MHC I-peptide complex dissociates, which causes unfolding, internalization and destruction of MHC I in endosomal compartments<sup>3</sup>. Newly produced MHC II molecules also associate constitutively with an endogenous ligand in the ER, in this case invariant chain (Ii), a chaperone that occupies the MHC-II molecule peptide-binding site to protect the site from premature association with ER-resident peptides. Ii also mediates transport of MHC II-Ii complexes to endosomal compartments. Extracellular proteins accessing these compartments are degraded by endolysosomal proteases, producing peptides that replace Ii in a reaction involving several proteases and chaperones<sup>4</sup>. CD1 molecules present lipids through a presentation pathway that shares features with both the MHC I and MHC II pathways<sup>5</sup>. Here, newly synthesized CD1 molecules constitutively bind endogenous lipids in the ER in a process aided by lipid transfer proteins. The resulting complexes traffic *via* the Golgi to the plasma membrane and are quickly endocytosed, accessing endosomal compartments where the endogenous ligands are exchanged for lipid Ags present in these compartments. The newly formed CD1-lipid Ag complexes recycle back to the cell surface, allowing CD1 molecules to present endocytosed lipid Ags of exogenous origin. Sorting motifs in the cytoplasmic tails of CD1 a-d isoforms determine differential intracellular trafficking pathways, thereby diversifying the endosomal compartments that are sampled by the CD1 family. Thus, MHC and CD1 molecules utilize a broad range of Ag presentation strategies characterized by their unique intracellular trafficking routes. Nevertheless, they all share a common feature, namely they constitutively

acquire self ligands in the ER soon after synthesis and traffic to the cell surface, where they are expressed at high levels for inspection by T cells, even in the absence of infection.

The MHC-I related molecule, MR1, presents a novel class of Ags released to the extracellular environment or the lumen of phagosomal compartments by microbes, consisting of derivatives of Vitamin B metabolism<sup>6, 7, 8, 9</sup>. These ligands (henceforth referred to as VitB Ags) are recognized bound to MR1 by mucosal associated invariant T (MAIT) cells<sup>7, 10, 11, 12</sup>. MAIT cells are highly abundant in humans, and although their role in health and disease remains unclear<sup>13, 14</sup>, their TCR-mediated activation and function is clearly dependent on MR1 Ag presentation. Thus, infections with microorganisms that produce VitB Ag ligands cause MAIT cell recruitment to and/or expansion at the site of infection in a MR1 dependent manner, but infections with microorganisms that do not produce the ligands do not trigger MAIT cell activation via the MAIT TCR<sup>15, 16, 17, 18</sup>.

Given the central role of presentation of pathogen-derived VitB Ag in MAIT cell function, it is important to characterize the intracellular mechanisms underpinning this activity. Presently it is established that MR1, while ubiquitously expressed in many cell types, is found on the cell surface at very low levels. In these conditions MR1 reportedly traffics through endosomal compartments, where it binds unknown ligands that are subsequently presented on the plasma membrane<sup>19</sup>. By extension, it is assumed that the route followed by MR1 for presentation of pathogen-derived ligands during infection also involves passage through endosomal compartments. Accessing these compartments would enable MR1 molecules to capture endocytosed VitB Ags, as is the case for presentation of exogenous peptide and lipid antigens by MHC II and CD1 molecules, respectively. The resulting MR1-VitB Ag complexes would then traffic to the plasma membrane leading to increased MR1 surface expression. However, whether this is the pathway followed by MR1 to acquire and present VitB Ags has not been investigated because this family of molecules has only recently been identified as the physiological pathogen-derived ligands of MR1<sup>6, 20</sup>. Accordingly, we determined the intracellular location where MR1 acquires VitB Ags, the trafficking pathway of the MR1-VitB Ag complexes and their fate after expression on the plasma membrane. Our results show that the site where MR1 binds VitB Ags is the ER, where most MR1 is retained in a ligand-receptive conformation, rather than bound to endogenous ligands, until suitable ligands capable of forming a Schiff base with the binding site of MR1 allows the resulting complexes to traffic from the ER to the cell surface.



## RESULTS

### A pre-synthesized intracellular pool of MR1 molecules capable of VitB Ag presentation

The VitB Ags acetyl-6-formyl pterin (Ac-6-FP) and 5-(2-oxopropylideneamino)-6-D-ribitylaminouracil (5-OP-RU) are MR1 ligands that potently induce upregulation of MR1 cell surface expression (**Figure 1a**)<sup>6, 7, 10</sup>. To establish whether the MR1 molecules expressed on cells incubated with 5-OP-RU or Ac-6-FP were indeed complexed to these ligands, we compared the levels of MR1 cell surface expression by FACS using two different reagents: a pan-MR1-specific mAb (26.5) and a newly generated soluble  $\alpha\beta$ TCR tetramer derived from a MAIT cell clone specific for MR1 associated to 5-OP-RU (**Figure 1b**). In conditions where cells expressed high levels of surface MR1 as detected with 26.5, only the cells exposed to 5-OP-RU bound the TCR tetramer (**Figure 1c**). This implied that the increase in MR1 surface expression induced by the ligands was attributable to their direct association to MR1, and not to an indirect induction of MR1 expression. Kinetically, MR1 surface expression was induced faster by 5-OP-RU than by Ac-6-FP, peaking at 4 and 8-16 hr, respectively (**Figure 1a**). C1R cells transfected to overexpress MR1 had similar cell surface expression kinetics to the endogenous MR1 (**Supplementary Figure 1**), whereas endogenous MHC I expression was not affected by culture with ligands (**Figure 1a**, **Supplementary Figure 1**). Interestingly, MR1 expression stabilized after the peak of induction in cells incubated continuously with Ac-6-FP but decreased in cells incubated with 5-OP-RU. This is attributable to Ac-6-FP being more stable in culture medium compared to 5-OP-RU (data not shown).

Notably, inhibiting protein exit from the ER/Golgi with brefeldin A (BFA) ablated the Ag-dependent increase in MR1 cell surface expression (**Figure 1a**). In contrast, inhibiting protein synthesis with cycloheximide (CHX) (**Figure 1d**) had a negligible effect on the initial upregulation of MR1, and only started to show an effect after 2 hr in cells incubated with Ac-6-FP and not at all in cells incubated with 5-OP-RU (**Figure 1a**). These observations were reproduced in primary human cells; MR1 cell surface expression was low on primary human peripheral blood mononuclear cells (PBMCs) and bronchial epithelial cells, but was up-regulated in the presence of 5-OP-RU in a process that was fully inhibited with BFA but not CHX (**Figure 1e**).

Next we tested the effect of BFA and CHX on MR1 presentation of natural riboflavin-based ligands produced by bacteria<sup>6, 7, 8, 9</sup>. Over 20% of C1R cells incubated with fluorescent (mCherry<sup>+</sup>) *Salmonella* Typhimurium (STM) strains SL1344 (wild type) or HW101 (riboflavin-pathway deficient) harbored fluorescent bacteria in intracellular vacuoles (**Figure 2a-b**). Overall surface MR1 expression was unaffected by infection (**Figure 2a**). This was unsurprising, as the amount of

ligand produced within the infected cells is likely too small to raise the rate of formation of new MR1-ligand complexes highly enough to cause a net increase in total surface MR1 detectable by flow cytometry. This result also suggested that bacterial invasion is insufficient to cause MR1 upregulation; rather, ligand availability appeared to be the limiting factor. To overcome the limitations of flow cytometry-based measurements, we resorted to a more sensitive assay to detect MR1 presentation of bacteria-derived ligands, namely activation of autologous MAIT cells recognizing MR1-Ag complexes on primary PBMCs<sup>11</sup>. This assay was at least 10-fold more sensitive than the flow-cytometry-based assay (**Figure 2c**). We infected adherent PBMCs with STM-SL1344 or HW101 in the presence or absence of BFA or CHX, and fixed the infected cells to prevent further changes to MR1 expression or antigen presentation. The efficiency of infection was not affected by BFA or CHX treatment (**Figure 2e**). Infected cells were then incubated with autologous PBMCs, and the activation of MAIT cells was assessed by measuring their production of TNF $\alpha$  (**Figure 2d-e**). MR1 presentation was profoundly inhibited if the antigen presenting cells had been treated with BFA, but much less so if the infected cells had been treated with CHX (**Figure 2e**). The effects of the two inhibitors on MAIT cell activation recapitulated those observed in measurements of presentation of MR1-Ag complexes by flow cytometry (**Figure 1a**).

These results suggest that in a diverse range of cell types, synthetic or bacteria-produced VitB Ags elicit egress of a pre-synthesized pool of MR1 molecules from a pre-Golgi compartment (the ER) to the plasma membrane. This pool was large enough to sustain upregulation of MR1 surface expression in cells incubated for 2-4 hr with VitB Ags, and for presentation of bacterial antigen to MAIT cells, in the presence of CHX, in which synthesis of new MR1 molecules was completely shutdown (**Figure 1d**). Of note, since ligand availability appeared to be the only factor required to induce MR1 expression on the cell surface, an implication of our observations is that, unlike MHC I or II, or CD1, MR1 molecules had little access to constitutively produced self ligands in the absence of infection. This was true not just for cells in culture but also for human PBMC.

### **MR1 molecules are retained within the ER in the absence of exogenous ligands**

To establish biochemically the origin and location of MR1 in cells before and after incubation with VitB Ags, we performed cell surface protein biotinylation followed by precipitation of biotinylated proteins and western blot of MR1. We performed this experiment firstly with C1R cells transfected with MR1 (C1R.MR1) to facilitate detection of the molecule. This confirmed that cells incubated with Ac-6-FP or 5-OP-RU, but not their counterparts incubated without ligands, contained detectable amounts of MR1 on their plasma membrane (**Figure 3a**, right). In contrast, analysis of total MR1 (either biotinylated or not) immunoprecipitated from cell lysates and visualized by

western blot revealed substantial amounts of the MR1 molecule in cells incubated without or with ligands (**Figure 3a**, left). To address our hypothesis that in the absence of ligands the MR1 molecules were located in a pre-Golgi compartment, we treated the immunoprecipitates with Endoglycosidase H (Endo H). This enzyme removes carbohydrates from glycoproteins that have not yet been processed during passage through the Golgi. All the MR1 molecules contained in cells incubated without ligands were sensitive to digestion with Endo H whereas most of their counterparts contained in cells incubated with Ac-6-FP or 5-OP-RU were resistant (**Figure 3a**, left). The small amount of Endo H-sensitive MR1 present in cells incubated with ligands were likely recently synthesized molecules that had not yet bound ligand and left the ER because all of the surface (biotinylated) MR1 in these cells was Endo H resistant (**Figure 3a**, right). Similar observations were made using human PBMC (**Figure 3b**), in which MR1 is expressed at much lower levels. The localization of MR1 was further analyzed using confocal microscopy, which showed almost complete co-localization of MR1 fused to green fluorescent protein (GFP) and an ER marker in cells not incubated with ligand, but MR1-GFP localization on the plasma membrane in cells incubated with Ac-6-FP (**Figure 3c**). MR1-GFP behaved similarly to wild-type MR1, remaining Endo H sensitive until MR1-GFP-expressing cells were incubated with ligands (**Supplementary Figure 2**). Our results indicated that in the absence of ligands MR1 is mostly retained in the ER independent of its level of expression, confirming the limiting factor that determines ER retention vs egress is ligand availability. As both cells in culture and PBMC retained in the ER most of their MR1 molecules, an important conclusion of these observations is that human cells do not produce significant amounts of self MR1 ligands in the steady state, nor do they obtain them from the extracellular environment, at least in blood, where the PBMC came from.

To analyze in further detail MR1 synthesis and trafficking out of the ER in the absence or presence of ligand, we assessed conversion of Endo H sensitive to resistant MR1 by metabolic radiolabelling (pulse) and chase experiments followed by immunoprecipitation, SDS-PAGE and autoradiography. Newly synthesized MR1 molecules were Endo H sensitive (**Figure 3d**) and remained so in the absence of ligand for the next 24 hr, a period during which the amount of radiolabeled MR1 gradually declined, indicative of degradation within the ER or via the ER-associated degradation (ERAD) pathway<sup>21</sup>. Addition of Ac-6-FP during the chase period promoted conversion of MR1 into the Endo H resistant form. Similar results were obtained in cells incubated with 5-OP-RU instead of Ac-6-FP (**Figure 3e**). The Endo H-resistant MR1 molecules were sensitive to PNGase F (**Figure 3e**), an enzyme that removes carbohydrates from glycoproteins, indicating that the post-translational modification that distinguished Endo H-sensitive MR1 molecules from their resistant counterparts indeed affected their carbohydrate moiety. The slow kinetics of degradation of radiolabelled MR1

in cells chased in the absence of VitB Ags is consistent with the conclusion that MR1 forms a stable pool of empty molecules in the ER. Interestingly, immunoprecipitation of MR1 from cells that had not been incubated with ligands retrieved little or no  $\beta$ 2m, but the MR1 molecules immunoprecipitated from cells incubated with Ac-6-FP or 5-OP-RU were associated with  $\beta$ 2m (**Figure 3a,b, and d**). This suggested that ligand encounter within the ER induced changes in MR1 conformation and promoted stable binding of  $\beta$ 2m, a possibility we further investigated in the following experiments.

### **Complete folding of MR1 requires formation of a Schiff base with VitB Ag**

The mAb 8F2.F9 reacts preferentially with fully folded MR1 molecules<sup>22</sup>, so we used this reagent to assess by immunoprecipitation and confocal microscopy the conformational state and location of MR1 in cells incubated with or without VitB Ags. Very little MR1 could be immunoprecipitated with 8F2.F9 from cells incubated without Ags even though a rabbit serum specific for the cytosolic tail of MR1 (capable of recognizing folded or unfolded molecules) retrieved abundant MR1 (**Figure 4a**). However, little  $\beta$ 2m co-precipitated with MR1 in these conditions (**Figure 4a**). Incubation of the cells with Ac-6-FP increased the amount of MR1 bound to  $\beta$ 2m that could be immunoprecipitated with the anti-cytosolic tail rabbit serum, and virtually all these molecules were 8F2.F9-reactive (**Figure 4a**). We also wanted to visualize in detail the localization of MR1 by confocal microscopy, and to enhance resolution of intracellular structures we used HeLa cells transfected with MR1. The analysis confirmed the absence of 8F2.F9-reactive molecules in cells incubated without MR1 ligands, but abundant expression of 8F2.F9-reactive MR1 decorating the plasma membrane in cells incubated with Ac-6-FP (**Figure 4b**). Strikingly, when egress of MR1 out of the ER was blocked with BFA, MR1 bound to  $\beta$ 2m could still be immunoprecipitated with 8F2.F9 from cells incubated with Ac-6-FP (**Figure 4a**), and these molecules accumulated in the ER (**Figure 4b**). These results imply that Ac-6-FP could access the ER and bind MR1 in this location, causing a conformational change in MR1 characterized by stable association with  $\beta$ 2m and acquisition of the 8F2.F9-reactive fold.

We next asked what was the molecular mechanism that triggered MR1 trafficking out of the ER in the presence of ligand. In the TCR-MR1-Ag crystal structures<sup>6, 7, 10, 12</sup>, the VitB Ags are located within the A'-pocket of the MR1 ligand binding site, surrounded by a large number of aromatic residues. At the base of this 'aromatic cradle' sits MR1 Lys43, which forms a Schiff base (a covalent bond) with bound ligands<sup>6, 8</sup>. We previously showed that mutating the Lys43 residue to Ala facilitates folding of recombinant MR1 *in vitro*<sup>23</sup>, so we reasoned that the intracellular formation of this covalent adduct between MR1 and the ligand might serve as a molecular trigger

for MR1 folding and egress out of the ER. To establish this we generated a Lys43Ala MR1 mutant, expressed it in C1R cells (C1R.MR1-K43A) and examined its expression and trafficking. Association to  $\beta$ 2m, acquisition of Endo H resistance and cell surface expression of MR1-K43A did not require incubation with VitB Ags (**Figure 4d**). We do not know if the MR1-K43A mutant molecule is expressed on the cell surface in empty form or bound to a putative endogenous ligand, but these findings demonstrate that MR1 remains incompletely folded within the ER unless its positively charged Lys43 is neutralized. To further test this hypothesis, we made a second mutant form of MR1 at position 43, in this case exchanging the Lys for Arg. While Arg has a long positively charged side chain like Lys, its capacity to form a Schiff base is severely diminished<sup>24</sup>, so in the mutant MR1-K43R molecule the positive charge of Arg43 cannot be neutralized by VitB Ags. C1R cells transfected with MR1-K43R contained a similar amount of MR1 as transfectants expressing the WT molecule (**Figure 4e**), but the mutant molecule did not become EndoH resistant, and it did not reach the cell surface, even after incubation with VitB Ag (**Figure 4f**). Our analysis confirms that the Lys43 residue in the wild-type molecule plays a key role regulating MR1 folding and expression. In its free state, Lys43 prevents complete folding of ligand-free MR1, but VitB Ag ligation serves as a “molecular switch” that neutralizes this positively charged residue, triggering complete MR1 folding around the ligand, association with  $\beta$ 2m and egress of the trimeric complex to the cell surface.

### **Most surface MR1-ligand complexes are endocytosed and degraded independently of ligand binding affinity**

We next addressed the fate of the MR1-ligand complexes. Ag-presenting molecules on the cell surface are ultimately re-internalised by endocytosis. Upon reaching early endosomes, two non-exclusive fates follow, namely recycling back to the cell surface, possibly following re-loading with new ligands acquired in endosomes, or trafficking to lysosomes for degradation. We aimed to establish the rate of endocytosis and the proportion of endocytosed molecules that recycled back to the cell surface. We incubated C1R.MR1 cells without or with ligands for 4 hrs and measured endocytosis of surface MR1 using an anti-MR1 mAb conjugated to a fluorescently labelled DNA-based internalisation probe (FIP assay<sup>25</sup>). This assay enables accurate measurements of surface molecule internalization across a wide range of levels of expression<sup>25</sup>. Approximately 50% of surface MR1 was internalized within 2-4 hrs independently of association with ligand (**Figure 5a**). Microscopy analysis confirmed transition of MR1 molecules labeled on the cell surface to intracellular structures within 1 hr (**Figure 5b**). Some of these structures co-labeled with early (EEA1+) or late (Lamp+) endosomal markers as expected (**Figure 5b**). The fraction of internalized MR1 molecules that recycled back to the surface was very small, and this was also independent of

whether the molecules were bound to VitB Ags (**Figure 5a**). This observation prompted us to examine whether surface MR1 molecules trafficking to endosomes and recycling back to the plasma membrane could efficiently present new ligands acquired during transit through endosomes, as other Ag presenting molecules do, particularly MHC II and CD1<sup>5, 26</sup>. This was a plausible hypothesis because, although MR1 and VitB Ags are covalently associated via Schiff base bonding, this link is labile at the moderately low pH (5-6) found in late endosomes.

First we determined whether MR1 molecules expressed on the plasma membrane of cells cultured in the absence of VitB Ags could bind ligands at this location. This was the case, because incubation of such cells with 5-OP-RU for 20 min at 4° C (to prevent internalization of surface molecules) led to formation of MR1-5-OP-RU complexes, detectable with TCR tetramer (**Figure 5c**). We then asked whether surface MR1 molecules that had already acquired ligands intracellularly were also receptive to 5-OP-RU. The answer was no, because cells pre-incubated with the VitB Ag 6-FP (a ligand that binds MR1 with lesser affinity than 5-OP-RU<sup>10</sup>) could not generate MR1-5-OP-RU complexes (**Figure 5c**). These observations indicated that the small amount of MR1 expressed on the surface of cells not incubated with VitB Ags are receptive to ligand binding at this location, presumably because they are empty or bound to a yet unknown ligand with very low affinity. However, molecules that acquired ligands intracellularly and then trafficked to the cell surface did not tolerate ligand replacement at this location, at least in the conditions tested here. To test whether these molecules could acquire ligands if they were allowed to undergo internalization and recycling, we incubated C1R.MR1 cells pre-exposed to 6-FP, to 5-OP-RU for 2 hr at 37°C. TCR tetramer staining confirmed formation of MR1-5-OP-RU complexes in these conditions (**Figure 5d**), but the complexes could have originated at two locations: within the ER, where 5-OP-RU could have bound newly synthesized MR1 molecules, or within the endocytic route, where 5-OP-RU could have replaced 6-FP in molecules recycled from the cell surface. We treated the cells with BFA to block the ER-derived source, finding that ~60% of the complexes generated during the assay required egress of molecules out of the ER. This contrasted with the measurement of 5-OP-RU presentation by cells that had not been pre-incubated with 6-FP (and expressed little MR1 on the surface): virtually all of the complexes presented in these conditions were derived from an ER source as BFA blocked their expression (**Figure 1a and 5d**). In conclusion, once a sufficiently high number of MR1 bound to VitB Ags has accumulated on the cell surface, these complexes can serve as a source of molecules for binding of new ligands in endosomal compartments and presentation upon recycling to the surface. This is a pathway that may enable presentation of MR1 ligands that cannot efficiently reach the ER. Nevertheless, the contribution of this pathway to MAIT cell activation *in vivo* remains uncertain, as the ER-based

pathway for MR1 presentation remains highly efficient even in cells that have already accumulated a large number of MR1-ligand complexes on their plasma membrane.

Finally we addressed what happened to MR1-mediated VitB Ag presentation after removal of the ligand from the extracellular environment. Cells that had been incubated overnight with 5-OP-RU, washed, and then placed in new medium devoid of the ligand immediately started to lose expression of MR1-5-OP-RU complexes, as measured by tetramer staining (**Figure 5e**). Similarly, MR1 molecules biotinylated at the cell surface were found to be steadily degraded over 8 hours (**Figure 5f**). This observation confirmed the rate of MR1 turnover is independent of ligand binding, and the level of presentation of a particular VitB Ag is strictly dependent on its availability for loading onto MR1 molecules. Collectively, the findings from this study illustrate that MR1 antigen presentation is characterized by a rapid “off-on-off” mechanism strictly dependent on antigen availability (**Supplementary Figure 3**).

## DISCUSSION

Peptides, lipids and small metabolites represent three classes of Ag that are presented by MHC, CD1 and MR1 molecules, respectively, for T cell surveillance<sup>1, 27, 28, 29</sup>. Each Ag presenting molecule utilizes distinct strategies to obtain, capture and present antigens for MHC and CD1. Here we show that the MR1 Ag presentation pathway possesses several features that sets it apart from the pathways used by other antigen-presenting molecules. Unlike MHC and CD1 molecules, most of the MR1 molecules synthesized by a cell do not constitutively associate with endogenous ligands (cytosolic peptides for MHC I, Ii for MHC II and lipids for CD1); instead they accumulate within the ER, in an incompletely folded conformation free of  $\beta 2m$ . It is at this location where they act as an ER-resident sensor of VitB Ags. Before encounter of such ligands, only a small fraction of MR1 molecules leave the ER and traffics to the cell surface, possibly via endocytic compartments as suggested in previous studies<sup>19</sup>. These MR1 molecules can bind extracellular ligands upon reaching the plasma membrane, indicating they are expressed in an empty form or bound to low-affinity endogenous ligands that can readily be replaced by VitB Ags. Nevertheless, the contribution of surface MR1 to VitB Ag presentation is very small.

The location where most of the MR1-VitB Ag complexes originate is the ER. This is another unique property that distinguishes MR1 from the two other molecules specialized in the presentation of extracellular antigens, namely MHC II and CD1, which capture their ligands in endosomal compartments. Formation of MR1-Vit B Ags in the ER implies the existence of a yet uncharacterized pathway for transfer of VitB Ags from the extracellular medium, or from the

interior of phagosomes harboring bacteria, to the ER lumen. It is in this location where the MR1 Ags sponsor, via formation of a Schiff base bond, complete folding of MR1, association with  $\beta 2m$  and trafficking of the ternary complex to the cell surface. Formation of a covalent bond (Schiff base) between MR1 and the ligands it presents is a third distinctive characteristic of MR1 as compared to other Ag-presenting molecules. All surface MR1-VitB Ag complexes are re-internalised with similar kinetics regardless of ligand binding, and most of these molecules are degraded instead of recycled. Thus, the MR1 presentation pathway acts as a quick sensor of extracellular VitB Ags, enabling rapid activation of MAIT cells and maintenance of Ag presentation for as long as the VitB Ag remain in the extracellular environment. Elimination of the source of VitB ligands is followed by a steady decline in the number of MR1-Ag complexes exposed on the cell surface for MAIT cell recognition.

An implication of our study is that the level of MR1 expression on the surface of cells in different anatomical locations is directly proportional to local antigen availability. Low MR1 expression on cells located in a sterile tissue such as the blood (PBMC) is consistent with this notion. An interesting question is whether such level is sufficient to drive MAIT cell selection in the thymus. If it is not, an interesting possibility is that some antigen presenting cells in the thymus do express, or collect from the extracellular environment, some self MR1 ligand capable of inducing a higher level of expression. Addressing this important question will require analysis of thymic Ag-presenting cells.

In conclusion, the MR1 Ag presentation pathway follows distinct rules that set it apart from the other mechanisms of Ag presentation in humans, namely those carried out by MHC and CD1 molecules. The results presented here provide a framework for future studies aimed at characterizing the machinery responsible for retention of ligand-free MR1 molecules in the ER, transport of extracellular VitB Ags to the ER, and internalization and degradation of MR1-Ag complexes from the plasma membrane. The components of this machinery represent potential targets for therapeutic manipulation of the MR1-MAIT cell axis.



## **ACKNOWLEDGMENTS**

This research was supported by the National Health and Medical Research Council (NHMRC) and the Australian Research Council. JAV is a Principal Research Fellow of the NHMRC; DPF is an NHMRC SPRF; JR is an NHMRC Australia Fellow. We thank Prof. Ted Hansen and Dr. Wei-Jen Chua Yankelevich for the gift of the 8F2.F9 hybridoma, Claire Dumont for assistance with the internalisation and recycling assays, Dr. Hugh Reid for assistance in cloning the MR1 K43R mutant, Dr. Sarah Londrigan for assistance with the bronchial epithelial cells, and the Biological Optical Microscopy Platform (University of Melbourne) for microscopy expertise.

## REFERENCES

1. Rossjohn J, Gras S, Miles JJ, Turner SJ, Godfrey DI, McCluskey J. T cell antigen receptor recognition of antigen-presenting molecules. *Annu Rev Immunol* 2015, **33**: 169-200.
2. Pamer E, Cresswell P. Mechanisms of MHC class I--restricted antigen processing. *Annu Rev Immunol* 1998, **16**: 323-358.
3. Heemels MT, Ploegh H. Generation, translocation, and presentation of MHC class I-restricted peptides. *Annu Rev Biochem* 1995, **64**: 463-491.
4. Villadangos JA. Presentation of antigens by MHC class II molecules: getting the most out of them. *Mol Immunol* 2001, **38**(5): 329-346.
5. Barral DC, Brenner MB. CD1 antigen presentation: How it works. *Nature Reviews Immunology* 2007, **7**(12): 929-941.
6. Corbett AJ, Eckle SB, Birkinshaw RW, Liu L, Patel O, Mahony J, *et al.* T-cell activation by transitory neo-antigens derived from distinct microbial pathways. *Nature* 2014, **509**(7500): 361-365.
7. Kjer-Nielsen L, Patel O, Corbett AJ, Le Nours J, Meehan B, Liu L, *et al.* MR1 presents microbial vitamin B metabolites to MAIT cells. *Nature* 2012, **491**(7426): 717-723.
8. McWilliam HE, Birkinshaw RW, Villadangos JA, McCluskey J, Rossjohn J. MR1 presentation of vitamin B-based metabolite ligands. *Curr Opin Immunol* 2015, **34C**: 28-34.
9. Eckle SB, Corbett AJ, Keller A, Chen Z, Godfrey DI, Liu L, *et al.* Recognition of Vitamin B precursors and byproducts by Mucosal Associated Invariant T cells. *The Journal of biological chemistry* 2015.
10. Eckle SB, Birkinshaw RW, Kostenko L, Corbett AJ, McWilliam HE, Reantragoon R, *et al.* A molecular basis underpinning the T cell receptor heterogeneity of mucosal-associated invariant T cells. *The Journal of experimental medicine* 2014, **211**(8): 1585-1600.
11. Reantragoon R, Kjer-Nielsen L, Patel O, Chen Z, Illing PT, Bhati M, *et al.* Structural insight into MR1-mediated recognition of the mucosal associated invariant T cell receptor. *The Journal of experimental medicine* 2012, **209**(4): 761-774.
12. Patel O, Kjer-Nielsen L, Le Nours J, Eckle SBG, Birkinshaw R, Beddoe T, *et al.* Recognition of vitamin B metabolites by mucosal-associated invariant T cells. *Nature Communications* 2013, **4**.
13. Gapin L. Check MAIT. *J Immunol* 2014, **192**(10): 4475-4480.
14. Gold MC, Lewinsohn DM. Co-dependents: MR1-restricted MAIT cells and their antimicrobial function. *Nature Reviews Microbiology* 2013, **11**(1): 14-19.
15. Sakala IG, Kjer-Nielsen L, Eickhoff CS, Wang X, Blazevic A, Liu L, *et al.* Functional Heterogeneity and Antimycobacterial Effects of Mouse Mucosal-Associated Invariant T Cells Specific for Riboflavin Metabolites. *J Immunol* 2015, **195**(2): 587-601.

16. Soudais C, Samassa F, Sarkis M, Le Bourhis L, Bessoles S, Blanot D, *et al.* In Vitro and In Vivo Analysis of the Gram-Negative Bacteria-Derived Riboflavin Precursor Derivatives Activating Mouse MAIT Cells. *J Immunol* 2015, **194**(10): 4641-4649.
17. Gold MC, Cerri S, Smyk-Pearson S, Cansler ME, Vogt TM, Delepine J, *et al.* Human mucosal associated invariant T cells detect bacterially infected cells. *PLoS Biol* 2010, **8**(6): e1000407.
18. Le Bourhis L, Martin E, Peguillet I, Guihot A, Froux N, Core M, *et al.* Antimicrobial activity of mucosal-associated invariant T cells. *Nature immunology* 2010, **11**(8): 701-708.
19. Huang S, Gilfillan S, Kim S, Thompson B, Wang X, Sant AJ, *et al.* MR1 uses an endocytic pathway to activate mucosal-associated invariant T cells. *J Exp Med* 2008, **205**(5): 1201-1211.
20. Kjer-Nielsen L, Patel O, Corbett AJ, Le Nours J, Meehan B, Liu L, *et al.* MR1 presents microbial vitamin B metabolites to MAIT cells. *Nature* 2012, **491**(7426): 717-723.
21. Ahner A, Brodsky JL. Checkpoints in ER-associated degradation: excuse me, which way to the proteasome? *Trends Cell Biol* 2004, **14**(9): 474-478.
22. Chua WJ, Kim S, Myers N, Huang S, Yu L, Fremont DH, *et al.* Endogenous MHC-related protein 1 is transiently expressed on the plasma membrane in a conformation that activates mucosal-associated invariant T cells. *J Immunol* 2011, **186**(8): 4744-4750.
23. Reantragoon R, Corbett AJ, Sakala IG, Gherardin NA, Furness JB, Chen Z, *et al.* Antigen-loaded MR1 tetramers define T cell receptor heterogeneity in mucosal-associated invariant T cells. *Journal of Experimental Medicine* 2013, **210**(11): 2305-2320.
24. Morris AJ, Davenport RC, Tolan DR. A lysine to arginine substitution at position 146 of rabbit aldolase A changes the rate-determining step to Schiff base formation. *Protein Engineering* 1996, **9**(1): 61-67.
25. Liu H, Johnston APR. A programmable sensor to probe the internalization of proteins and nanoparticles in live cells. *Angewandte Chemie - International Edition* 2013, **52**(22): 5744-5748.
26. Neefjes J, Jongsma ML, Paul P, Bakke O. Towards a systems understanding of MHC class I and MHC class II antigen presentation. *Nat Rev Immunol* 2011, **11**(12): 823-836.
27. Godfrey DI, Uldrich AP, McCluskey J, Rossjohn J, Moody DB. The burgeoning family of unconventional T cells. *Nature immunology* 2015, **16**(11): 1114-1123.
28. Van Rhijn I, Godfrey DI, Rossjohn J, Moody DB. Lipid and small-molecule display by CD1 and MR1. *Nat Rev Immunol* 2015, **15**(10): 643-654.
29. Rossjohn J, Gras S, Miles JJ, Turner S, Godfrey DI, McCluskey J. T cell antigen receptor recognition of antigen-presenting molecules. *Annual Review of Immunology* 2015, **In press**.
30. Holst J, Szymczak-Workman AL, Vignali KM, Burton AR, Workman CJ, Vignali DA. Generation of T-cell receptor retrogenic mice. *Nat Protoc* 2006, **1**(1): 406-417.

31. Huang S, Gilfillan S, Cella M, Miley MJ, Lantz O, Lybarger L, *et al.* Evidence for MR1 antigen presentation to mucosal-associated invariant T cells. *The Journal of biological chemistry* 2005, **280**(22): 21183-21193.
32. Tilloy F, Treiner E, Park SH, Garcia C, Lemonnier F, de la Salle H, *et al.* An invariant T cell receptor alpha chain defines a novel TAP-independent major histocompatibility complex class Ib-restricted alpha/beta T cell subpopulation in mammals. *The Journal of experimental medicine* 1999, **189**(12): 1907-1921.
33. Hoiseth SK, Stocker BA. Aromatic-dependent Salmonella typhimurium are non-virulent and effective as live vaccines. *Nature* 1981, **291**(5812): 238-239.
34. Datsenko KA, Wanner BL. One-step inactivation of chromosomal genes in Escherichia coli K-12 using PCR products. *Proceedings of the National Academy of Sciences of the United States of America* 2000, **97**(12): 6640-6645.
35. Strugnell R, Dougan G, Chatfield S, Charles I, Fairweather N, Tite J, *et al.* Characterization of a Salmonella typhimurium aro vaccine strain expressing the P.69 antigen of Bordetella pertussis. *Infect Immun* 1992, **60**(10): 3994-4002.
36. Reuter A, Panozza SE, Macri C, Dumont C, Li J, Liu H, *et al.* Criteria for dendritic cell receptor selection for efficient antibody-targeted vaccination. *J Immunol* 2015, **194**(6): 2696-2705.

## FIGURE LEGENDS

### **Figure 1. MR1 is recruited to the cell surface from a pre-synthesised intracellular pool.**

**a.** MR1 cell surface expression in C1R cells over time measured with mAb 26.5 by flow cytometry, with MHC-I expression for comparison, and represented as geometric mean fluorescence intensity (gMFI)  $\pm$  standard error of the mean (SEM). Cells were incubated with no ligand (upper graph) or with 10  $\mu$ M Ac-6-FP (middle) or 5-OP-RU (lower), in the presence of brefeldin A (red lines), cycloheximide (blue lines) or without inhibitors (black lines). Data shown is representative of three independent experiments.

**b.** SDS-PAGE of *E. coli*-expressed TCR  $\alpha$ - and  $\beta$ -chains of the MAIT TCR (upper panel). Non-reducing peak fraction lane 1, all fractions reducing lanes 3-8, including as a control 2  $\mu$ g of reduced previously-generated irrelevant TCR (lane 2). SDS-PAGE of biotinylated and multimerised MAIT TCR (middle panel). Streptavidin alone (lane 1), TCR alone (lane 2), biotinylated TCR (lane 3) and multimerised TCR (lane 4). MonoQ anion exchange chromatography was used to purify biotinylated TCR (lower panel).

**c.** C1R cells and C1Rs overexpressing MR1 (C1R.MR1) cultured without added ligand (black) or with 100  $\mu$ M Ac-6-FP (orange), 6-FP (orange dotted) or 5-OP-RU (red) for 4 hr, then stained for total surface MR1 with monoclonal antibody 26.5 (lower) or for MR1-5-OP-RU using a MAIT TCR tetramer (upper) and analysed by flow cytometry. MR1-5-OP-RU staining was blocked by mAb 26.5 (red filled histogram) and streptavidin-PE alone (SaV-PE; grey) or isotype control (grey) are shown for comparison. Data shown is representative of three independent experiments.

**d.** C1R.MR1 were pulsed for 30 min with  $^{35}$ S-labelled methionine/cysteine in the presence (+) or absence (-) of 20  $\mu$ g/ml cycloheximide (CHX), and MR1 was immunoprecipitated, and separated by reducing 11.5% SDS-PAGE. Radiolabelled proteins were detected by autoradiography film.

**e.** MR1 surface expression in freshly purified primary human peripheral blood mononuclear cells and in cultured normal human bronchial epithelial cells by mAb 8F2.F9 and flow cytometry. Cells were cultured without ligand (black line) or with 10  $\mu$ M 5-OP-RU (red line) for 4 hr, in the presence or absence of cycloheximide or brefeldin A. For comparison the 8F2.F9 mAb blocked by pre-incubation with soluble recombinant MR1-5-OP-RU (grey histogram) is shown. Similar results were obtained from at least two healthy donors.

### **Figure 2. Presentation of ligands produced by intracellular bacteria**

**a.** C1R cells were infected for 1 hr with mCherry<sup>+</sup> *Salmonella* Typhimurium (STM) strains SL1344 (wild type) or HW101 (MR1 ligand-deficient) at MOI 50. Upper panels show the percentage of

infected (mCherry<sup>high</sup>; red) or uninfected (mCherry<sup>low</sup>; black) cells. Surface MR1 on C1R cells following infection was measured by flow cytometry and is shown for infected (red) or uninfected (black) cells in the lower graphs. Data represents two independent experiments.

**b.** C1R.MR1 cells, which express GFP throughout the cytosol and nucleus, were infected with STM-SL1344 and analysed by fluorescence microscopy. Intra-vacuolar bacteria are indicated with white arrows.

**c.** C1R cells were incubated with the indicated concentration of 5-OP-RU for 4 hr then stained for surface MR1 levels (black), or fixed and then incubated with Jurkat.MAIT cells overnight. Activation of Jurkat.MAIT cells was measured by CD69 upregulation (red).

**d.** Adherent PBMCs were infected with STM HW101 or STM-SL1344 in the presence or absence of BFA or CHX, at MOI 50 for 5 hours. Cells were washed, fixed and incubated with live PBMCs from matching donors for 1 hr in the absence and for 6 hr additional in the presence of BFA. The percentage of MAIT cells (CD3<sup>+</sup> TRAV1-2<sup>+</sup> and MAIT-tetramer<sup>+</sup>) producing TNF $\alpha$  was determined by flow cytometry. Results for one representative donor of three are shown.

**e.** The summary of three donors' activation assays as described in d are shown as mean  $\pm$  SEM. The infection level of adherent PBMCs is represented as the proportion of mCherry<sup>+</sup> cells for each infection and treatment (left graph). The activation of MAIT cells (right graph) with each treatment is represented relative to activation without inhibitors.

### **Figure 3. MR1 is stored as an immature protein in the endoplasmic reticulum.**

**a.** C1R.MR1 cells were cultured for 6 hr without ligand or with 100  $\mu$ M Ac-6-FP or 5-OP-RU, and then cell surface proteins were biotinylated or left untreated. Cells were lysed and were immunoprecipitated (IP) with normal rabbit serum (NRS), anti-MR1-cytosolic tail polyclonal antibody (anti-MR1-CT) (left panel) or streptavidin (right panel) as indicated. Immunoprecipitates were treated with endoglycosidase H (endo H) or not and immunoblotted (IB) with anti-MR1-CT or anti- $\beta$ 2m mAb. Endo H-susceptible (S) or resistant (R) bands are indicated, and is a representative image of three independent experiments.

**b.** Freshly purified human PBMC were either immediately frozen ('no culture') or cultured for 12 hr with or without 100  $\mu$ M Ac-6-FP or 5-OP-RU, then lysed and immunoprecipitated as above. Shown is a representative of three healthy donors.

**c.** C1R cells overexpressing MR1 fused to green fluorescent protein (MR1-GFP; green) were cultured with or without 100  $\mu$ M Ac-6-FP for 18 hr, then incubated with an ER label (ER tracker; red) and imaged live using a confocal microscope. Colocalisation between MR1-GFP and ER tracker was measured by Pearson's correlation coefficient (PCC), and all are shown as mean  $\pm$  SEM.

SEM. Significant differences are indicated by the asterisks (\*\*\*\*;  $p < 0.0001$ ). Scale bar represents 5  $\mu\text{m}$ . Cells shown are maximum projections and represent two independent experiments.

**d-e.** C1R.MR1 were pulsed for 30 min with  $^{35}\text{S}$ -labelled methionine/cysteine and then chased for the indicated hours (h) with or without 100  $\mu\text{M}$  Ac-6-FP or 5-OP-RU. MR1 was immunoprecipitated with anti-MR1-CT, treated with or without Endo H or PNGase F, and separated by 11.5% SDS-PAGE, and is representative of two independent experiments for each.

#### **Figure 4. Ligands promote MR1 folding and ER release**

**a.** C1R.MR1 cells were incubated with or without 100  $\mu\text{M}$  Ac-6-FP and brefeldin A (BFA) for 6 hr, immunoprecipitated for MR1 by anti-MR1-CT or the conformational antibody 8F2.F9, and immunoblotted (IB) with anti-MR1-CT or anti- $\beta_2\text{m}$ . The image represents two independent experiments.

**b.** HeLa.MR1 cells grown on glass chamber slides were treated as above, then fixed with paraformaldehyde, permeabilised with saponin and stained for the ER marker BiP (green) and folded MR1 with 8F2.F9 (red). Scale bar represents 10  $\mu\text{m}$ . The intensity of 8F2.F9 staining was quantified and colocalisation between 8F2.F9-MR1 and BiP was measured by Pearson's correlation coefficient (PCC), and all are shown as mean  $\pm$  SEM. Significant differences are indicated by the asterisks (\*\*\*\*;  $p < 0.0001$ ). The images represent two independent experiments.

**c.** C1R.MR1 cells (wild type; WT) or cells transfected with MR1 mutated at Lys43 (MR1-K43A) were pulsed for 30 min with  $^{35}\text{S}$ -labelled methionine/cysteine and then chased for 0 or 6 hr with or without 100  $\mu\text{M}$  5-OP-RU. MR1 was immunoprecipitated with anti-MR1-CT, and samples were treated with or without Endo H. This represents two independent experiments.

**d.** C1R.MR1-WT or K43A cells were incubated  $\pm$  10  $\mu\text{M}$  Ac-6-FP for 6 hours, then surface MR1 was detected by flow cytometry using mAb 26.5, and represents three independent experiments.

**e.** MR1 cell surface expression in C1R cells transduced with either MR1-WT or MR1 mutated at Lys43 to Arg (MR1-K43R) over 4 hr with 10  $\mu\text{M}$  Ac -6-FP measured with mAb 26.5 by flow cytometry. Represented as geometric mean fluorescence intensity (gMFI)  $\pm$  standard error of the mean (SEM).

**f.** Total MR1 was immunoprecipitated from C1R cells transduced with MR1-WT or -K43R were cultured for 4 hr  $\pm$  100  $\mu\text{M}$  Ac -6-FP, treated with endoglycosidase H, and IB for MR1 (upper panel). To control for loading, 5% of the lysate ('input') was IB for actin (lower panel).

#### **Figure 5. Endocytosis and recycling of surface MR1**

**a.** The internalisation rate of surface MR1 was measured in C1R.MR1 cells with no ligand (black), or preloaded with 100  $\mu\text{M}$  Ac-6-FP (orange) or 5-OP-RU (red) for 4 hr (upper graph). Surface MR1

was labeled with anti-MR1 mAb 8F2.F9 conjugated to a specific hybridisation internalisation probe. Cells were allowed to internalise for up to 4 hr and any remaining surface fluorescence was quenched. Fluorescence of cells measured by flow cytometry indicates endocytosed MR1. The MR1 internalised was calculated as a percentage of the initial un-quenched signal. Recycling of internalised MR1 was measured (lower graph) by labeling surface MR1 with 8F2.F9-SS-biotin and allowing to internalise for 1 hr. Remaining biotin label at the surface was removed by a cell-impermeable reducing agent, and cells were then incubated for up to 1 hr to allow labeled MR1 to recycle back to the cell surface. Recycled MR1 was detected by incubating the cells with avidin conjugated to Alexa Fluor 647 and measured by flow cytometry. The amount of MR1 recycled was calculated as the percentage of the initial surface MR1 signal prior to biotin removal. For both assays, the mean of two independent experiments are shown with standard error of the mean.

**b.** HeLa.MR1 cells were pre-incubated for 16 hr with 100  $\mu$ M Ac-6-FP, then surface MR1 was labeled with 8F2.F9 conjugated to Alexa Fluor 647 (red). Cells were fixed or allowed to internalise for 1 hr before fixing. Representative cells from two experiments are shown, co-stained for EEA1 (upper panels; green) and LAMP1 (lower panels; green), and DAPI (blue) without internalization (0 hour) or after 1 hour at 37 °C. Each image is shown also without endosomal markers for clarity, and are maximum projections of seven Z-stacks through the centre of each cell. The boxed portion of 1 hour internalized images are shown on the right with endosomal MR1 co-staining with EEA1 or LAMP1 highlighted with white arrows. Scale bar is 10  $\mu$ m, and represents two independent experiments.

**c.** To measure loading of 5-OP-RU on cell-surface MR1, C1R.MR1 cells cultured without ligand (left graph) or preloaded for 4 hr with 20  $\mu$ M 6-FP (right graph) were incubated on ice with 100  $\mu$ M 5-OP-RU for 20 min (red line) or no ligand (black line). Cells were then stained with the MAIT TCR tetramer and compared to unstained cells (grey). This represents three independent experiments.

**d.** To measure exchange of 6-FP for 5-OP-RU by MR1, cells were treated as above and then cultured for 2 hr at 37 °C in the presence of 100  $\mu$ M 5-OP-RU (red solid line) or with 5-OP-RU and brefeldin A (BFA) (red dashed line), and then were stained with the MAIT TCR tetramer. The geometric mean fluorescence intensity (gMFI) from two independent experiments for both **c** and **d** is shown in the bar graphs (far right) +/- SEM.

**e.** C1R.MR1 cells were incubated for 16 hr with 100  $\mu$ M 5-OP-RU, washed three times and further incubated in media devoid of 5-OP-RU for the indicated times. Surface MR1-5-OP-RU was then measured by the MAIT TCR tetramer. Shown is a representative of three experiments.

**f.** C1R.MR1 cells were incubated for 16 hr with 100  $\mu$ M 5-OP-RU or Ac-6-FP, and surface proteins were biotinylated. Cells were cultured in fresh media for the indicated times, at which point they



were washed and lysed. Lysate was used directly for immunoblotting for actin determination (lower blot) or biotinylated proteins were immunoprecipitated using streptavidin-agarose. MR1 was detected by immunoblotting.

## ONLINE MATERIALS AND METHODS

### Cell lines and transfectants expressing wild-type or mutant MR1

C1R and HeLa cell lines expressing MR1 under the control of the p-MSCV-IRES-eGFP (pMIG<sup>30</sup>) vector were previously described<sup>11</sup>. The MR1-K43A mutant was previously generated<sup>11</sup> was also cloned into pMIG. A construct expressing MR1, or mutants thereof, fused to enhanced green fluorescent protein (GFP) at the C-terminus was generated by removing the IRES-GFP segment of pMIG and cloning in the MR1-GFP sequence. These constructs were transduced into C1R cells and sorted based on GFP level as a surrogate marker of MR1 expression.

Since cell culture media is a source of folate-derived MR1 ligands<sup>7</sup>, during experimental procedures cells were cultured in folate-free RPMI (Life Technologies), but were otherwise normally maintained in folate-sufficient media.

### Antibodies

For flow cytometry staining of MR1 the 26.5 mAb<sup>31</sup> was used, except for primary human cells where significant non-specific staining was observed with this clone. In this case the 8F2.F9 mAb<sup>22</sup> was used. MHC I was measured by flow cytometry using anti HLA class I-APC conjugate (clone Tü149; Life Technologies). A polyclonal rabbit antiserum was generated against a peptide corresponding to the final 15 residues of human MR1 cytosolic tail (PREQNGAIYLPTPDR) (anti-MR1-CT; Abmart). For immunoblot detection of  $\beta_2$ -microglobulin clone BBM.1 was used. The following antibodies were used to stain human PBMCs: anti CD19-FITC (BD; clone HIB19); anti CD3-Pacific blue (BD; clone UCHT1); anti CD14-Brilliant violet 570 (BioLegend; clone M5E2); anti TRAV1-2-APC (BioLegend; clone 3C10). MAIT cells were stained with PE-labelled tetrameric human MR1-5-OP-RU at 0.7  $\mu$ g/ml. For intracellular cytokine staining, cells were fixed for 20 min on ice with 1% paraformaldehyde (PFA), 2% glucose in PBS, then permeabilised and stained in 0.3% saponin/PBS with anti TNF $\alpha$  –Pacific blue (BioLegend; clone mAb11) overnight.

### MR1 ligands

MR1 ligands were added directly to the culture medium at the indicated concentrations: Ac-6-FP (Schircks Laboratories) and 5-OP-RU (by adding 5-A-RU<sup>6</sup> and methyl glyoxal (pyruvaldehyde; Sigma-Aldrich) at equimolar concentrations). The inhibitors cycloheximide and brefeldin A (Abcam) were used at 20  $\mu$ g/ml and 10  $\mu$ g/ml respectively.

### **MR1 surface expression by flow cytometry.**

C1R cells, freshly purified peripheral blood mononuclear cells from healthy donors, and normal human bronchial epithelial cells (Lonza) were cultured for the indicated time points with ligands and/or inhibitors. Cells were stained with the respective biotinylated mAbs followed by PE-conjugated streptavidin (Biolegend), and detected by flow cytometry. Propidium iodide was used to exclude dead cells. To demonstrate specific binding to MR1 in primary cells the mAb 8F2.F9 was blocked by pre-incubating with recombinant soluble human MR1-5-OP-RU generated as previously described<sup>6</sup> (10:1 molar ratio). To measure surface expression of MR1-5-OP-RU complexes, a MAIT TCR tetramer was generated based on TRBV6-1<sup>+</sup> MAIT TCR (clone A-F7)<sup>32</sup>, conjugated to PE and used at 5 µg/ml. Briefly, TCR α-chain was mutated to express a C-terminal Cys, TCR α- and β-chains were expressed, refolded and purified as described previously<sup>10, 12</sup>, then biotinylated using the EZ-Link Maleimide-PEG2-Biotin Kit (ThermoFisher). Biotinylated TCR was isolated from non-biotinylated species by MonoQ anion exchange chromatography and conjugated to Streptavidin-Fluorochrome (BD).

### ***Salmonella* Typhimurium strains**

Bacterial infections were carried out with *Salmonella enterica* var Typhimurium (STM) ‘wild-type’ strain SL1344<sup>33</sup>. For the ligand-deficient strain (HW101), ΔribDH mutants were constructed on an SL1344 background by lambda-red-recombinase-mediated allelic replacement<sup>34</sup> followed by general transduction using phage P22 as described<sup>35</sup>, and was grown in media supplemented with 20 µg/ml riboflavin. Strains carrying stable chromosomal expression of mCherry were generated using P22-mediated phage transduction of mCherry chromosomal integrants very kindly provided by Dr. Leigh Knodler, Paul Allen School for Global health, Washington State University College of Veterinary Medicine, USA.

### **MAIT cell activation assays**

C1R cells were infected for 1 hour at MOI 50 then washed and cultured for up to 6 hours in the presence of gentamycin (40 µg/ml). For the comparison of MR1 surface expression and activation for a range of 5-OP-RU concentrations, C1R cells were incubated with titrating amounts of 5-OP-RU were fixed for 20 min on ice with 1% PFA, 2% glucose in PBS, then washed 3 times with media and cultured with Jurkat cells transduced with a MAIT TCR<sup>7</sup> (Jurkat.MAIT) over night.

For human PBMC activation assays, whole PBMCs were cultured in plastic plates for 2 hr, then non-adherent cells were removed and cultured overnight until the activation assay. Adherent PBMCs were washed and infected with STM strains for 5 hours in the presence or absence of BFA

(10 µg/ml) or CHX (20 µg/ml), after which time they were fixed as above and incubated with the matching non-adherent PBMCs from the same donor for 1 hr, then a further 6 hr in the presence of BFA.

### **Immunoprecipitations and cell surface biotinylation**

For immunoblotting and detection of MR1, cells were lysed in 0.5 % IGEPAL CA-630 (Sigma-Aldrich), 50 mM Tris-Cl pH 7.4, 5 mM MgCl<sub>2</sub> with Complete Protease Inhibitor cocktail (Roche), and nuclei were separated by centrifugation at 13,000 x g for 10 min. Lysates were pre-cleared with normal rabbit serum (Sigma-Aldrich) and protein G sepharose, then a second time with protein G sepharose alone. MR1 was immunoprecipitated using anti-MR1-CT and protein G sepharose, and precipitates were washed three times with NET buffer (0.5 % IGEPAL CA-630, 50 mM Tris-Cl pH 7.4, 150 mM NaCl, 5 mM EDTA) and treated with Endoglycosidase Hf (New England Biolabs) as per the manufacturer's instructions. Proteins were denatured with reducing SDS-PAGE sample buffer, separated on NuPAGE 4-12% Bis-Tris pre-cast gels (Life Technologies) and immunoblotted on to nitrocellulose membranes using the iBlot system (Life Technologies). To detect MR1 in primary human PBMCs 100 million cells were used per immunoprecipitation, whereas for C1R.MR1 cells only 1 million were required. For biotinylation of cell surface proteins cells were washed twice in PBS (pH 8) and resuspended in the cell-impermeable EZ-link Sulfo-NHS-Biotin (0.25 mg/ml, PBS pH 8; Thermo Scientific) for 30 min on ice. Cells were washed in 0.1 M glycine/PBS twice then lysed as above, and immunoprecipitated using streptavidin agarose (Pierce).

### **Radiolabelling**

Cells were starved for 30 min in media methionine and cysteine free DMEM, then pulsed for 30 min in this media supplemented with 35S-labelled methionine/cysteine (Express Protein Labelling Mix, Perkin Elmer) at 200 µCi/ml. Cells were washed and then chased in folate-free RPMI-1640 for the indicated times, then washed in PBS and frozen. Cells were lysed and immunoprecipitated as above with an additional pre-clear step of protein G sepharose. Precipitates were washed 3 times in NET buffer containing 0.2% SDS, and treated with endoglycosidase Hf or PNGase F (New England Biolabs) as per the manufacturer's instructions. Proteins were separated by 11.5% SDS-PAGE, and gels were rinsed in DMSO and then in 22% 2,5-diphenyloxazole/DMSO followed by water, then dried and exposed to Hyperfilm MP (GE Healthcare).

### **Confocal microscopy**

For imaging MR1-GFP in C1R cells, after overnight culture with Ac-6-FP cells were washed once in Hanks Balanced Salt Solution and incubated with 200 nM ER-Tracker Blue-White DPX (Life

Technologies) for 15 min at 37 °C, washed and imaged live using a Zeiss LSM710 confocal microscope.

HeLa.MR1 cells were grown overnight on Lab-Tek chamber slides (Nunc), and following treatments were fixed with 4% paraformaldehyde in PBS. Cells were blocked and permeabilised with 10% normal donkey serum and 0.05% saponin, and incubated with primary antibodies diluted in blocking buffer against MR1 (mAb 8F2.F9 2 µg/ml) and rabbit anti-BiP/GRP78 (Abcam, 1:200). After two washes in PBS, Alexa Fluor 568-conjugated anti-rabbit IgG and Alexa Fluor 647-conjugated anti-mouse IgG in blocking buffer were added. Finally cells were washed in PBS and incubated with 4',6-diamidino-2-phenylindole (DAPI, 1 µg/ml) for 5 min followed by mounting in 90% glycerol, 20 mM Tris-Cl pH 8, 0.2M DABCO.

For visualising endocytosed MR1 HeLa.MR1 cells were incubated with Ac-6-FP for 16 hours then surface MR1 was labelled using Alexa Fluor 647-conjugated 8F2.F9 for 20 min on ice, then washed and either fixed directly in 4% PFA or cultured to allow internalisation of MR1 for 1 hour then fixed. Cells were stained as above for goat anti-EEA1 (Santa Cruz) or rabbit anti-LAMP1 (Abcam), followed by either Alexa Fluor 568-conjugated anti-goat or rabbit IgG, respectively.

Colocalisation analysis was performed on 12-20 individual cells selected at random, using Imaris (8.1.2 Bitplane), and the automatic threshold function was used to calculate the thresholded Pearson's correlation coefficient. To assess the mean staining intensity with mAb 8F2.F9, the mean fluorescence signal was measured for each cell using Imaris. For statistical analysis two groups were compared using the Mann-Whitney test, and for more than two groups the Kruskal-Wallis test with multiple comparisons was employed (Prism 6, GraphPad).

### **Internalisation assay**

To measure MR1 internalisation a fluorescence internalisation probe (FIP) using mAb 8F2.F9 was generated as described by Reuter and Panozza et al.<sup>36</sup>. Briefly, the FIP conjugated to 8F2.F9 contains a DNA sequence conjugated to the fluorescent dye Cy5, which can be quenched by use of a quencher conjugated to the complementary DNA sequence. Any Cy5 signal not quenched indicates protection due to internalisation. Cells were labelled with 8F2.F9-FIP on ice, then washed and incubated at 37 °C for the indicated time points when they are placed on ice to halt internalisation. Cells were washed and resuspended with or without the quencher, and Cy5 fluorescence analysed by flow cytometry. The Cy5 signal remaining after quenching indicates internalised MR1, and was calculated as a percentage of the initial signal prior to internalisation.

### **Recycling assay**

The mAb 8F2.F9 was conjugated to NHS-SS-Biotin (Thermo Scientific) to create a cleavable biotin tag. Cells were incubated with this on ice, then washed and allowed to internalise at 37 °C for 1 hour. Cells were then treated with 100 mM sodium 2-mercaptoethanesulfonate (Sigma) in 50 mM Tris-Cl pH 8.6, 150 mM NaCl, 1mM EDTA to cleave biotin from exposed non-internalised 8F2.F9, twice for 10 min. After washing, cells were cultured for up to 1 hour to allow recycling of endocytosed 8F2.F9 to the cell surface. Finally cells were washed and stained with Alexa Fluor 647-conjugated streptavidin to detect recycled MR1, and measured by flow cytometry. The amount of MR1 recycled was calculated as the percentage of the initial surface MR1 signal prior to biotin removal.

**Figure 1**

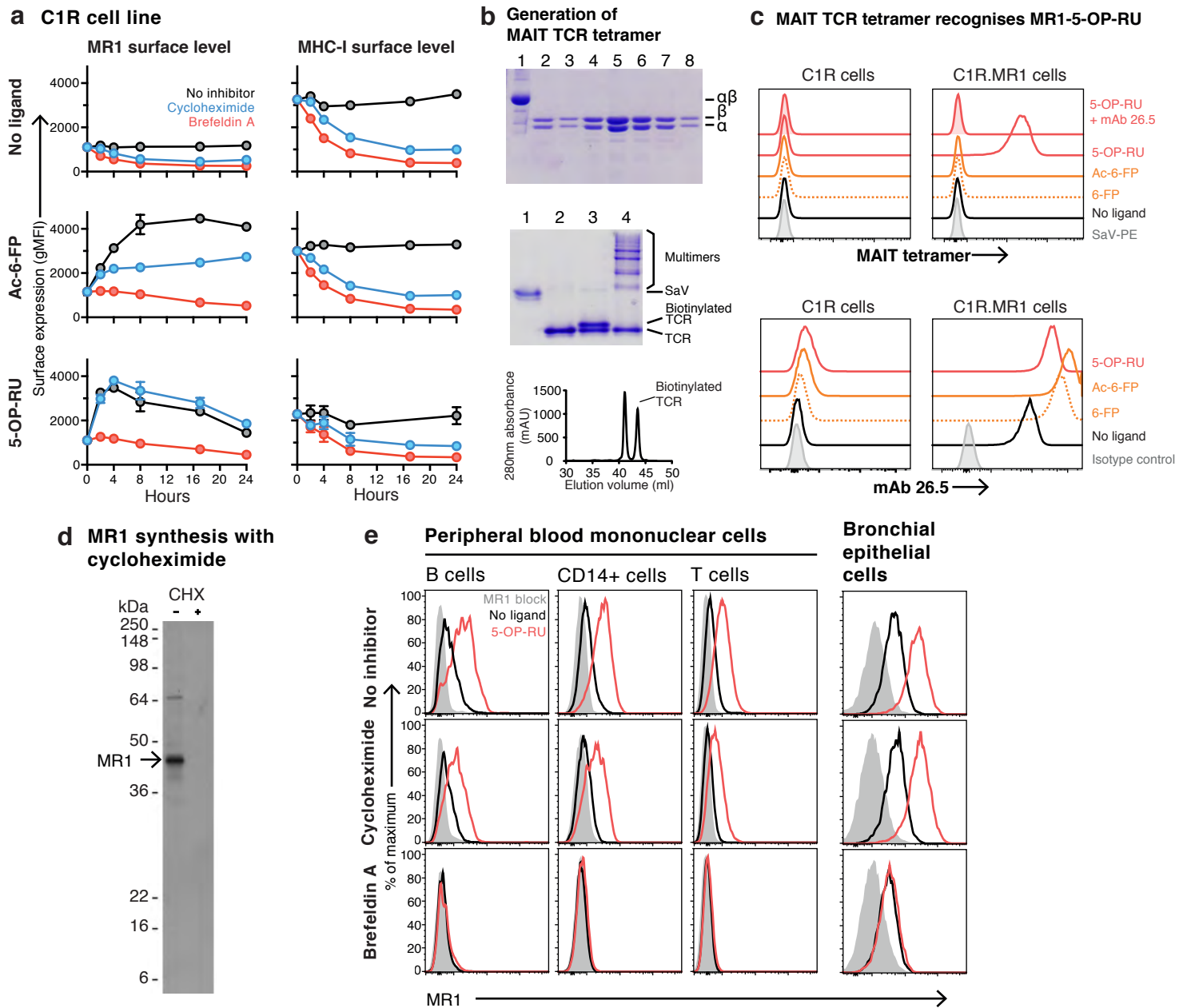


**Figure 2**

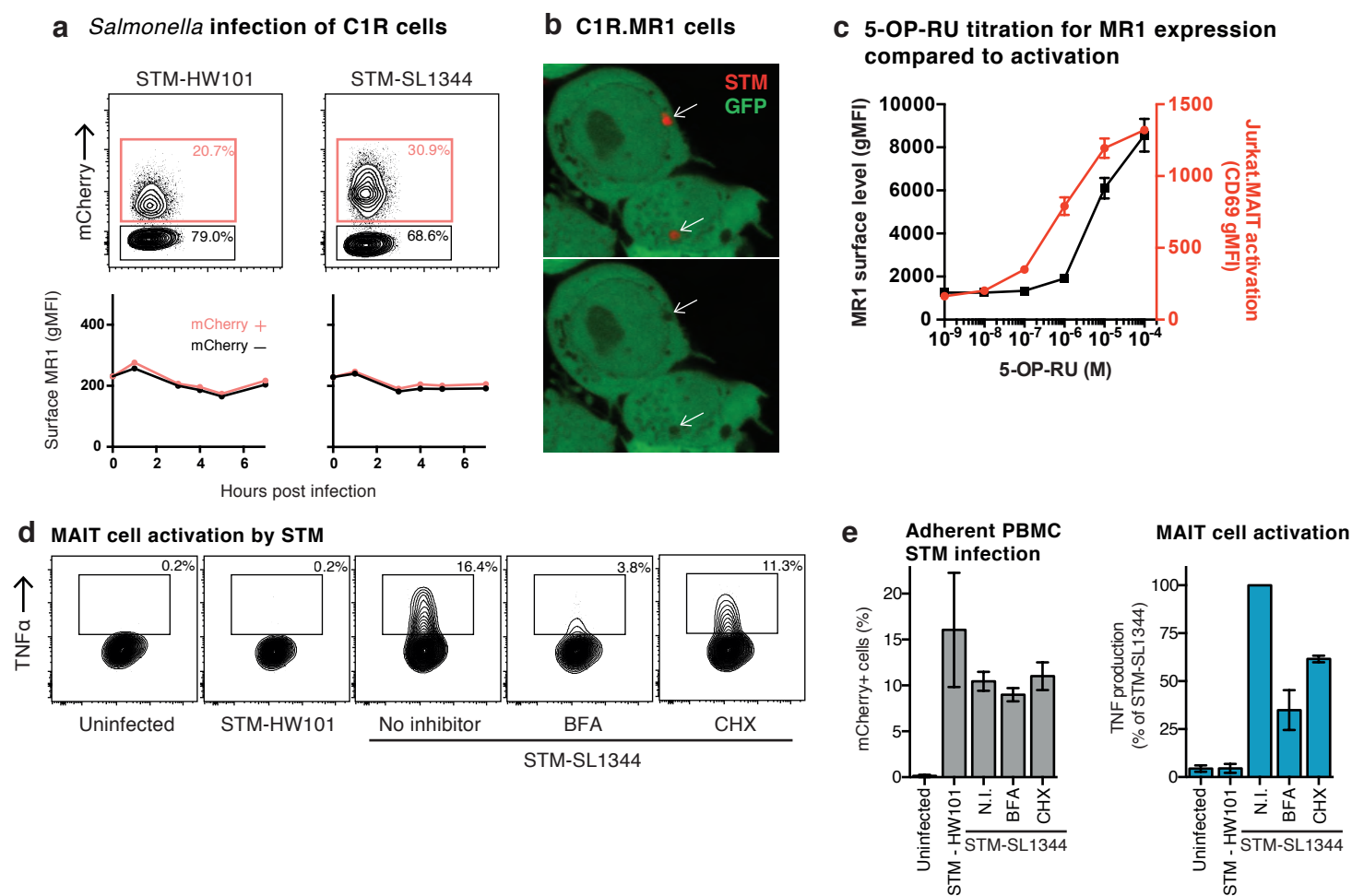
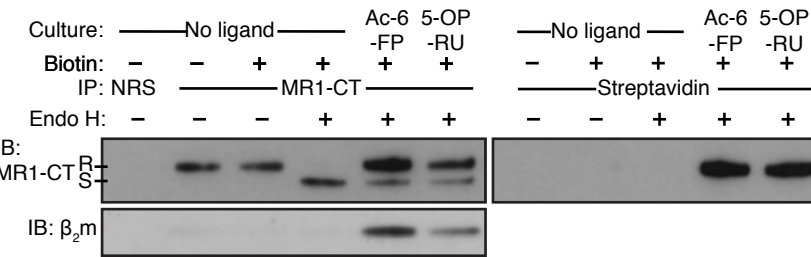


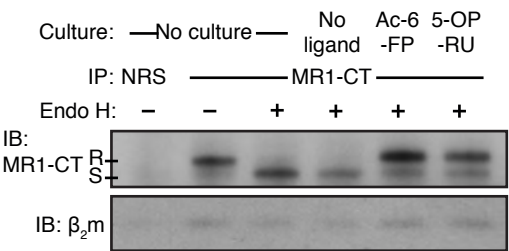


**Figure 3**

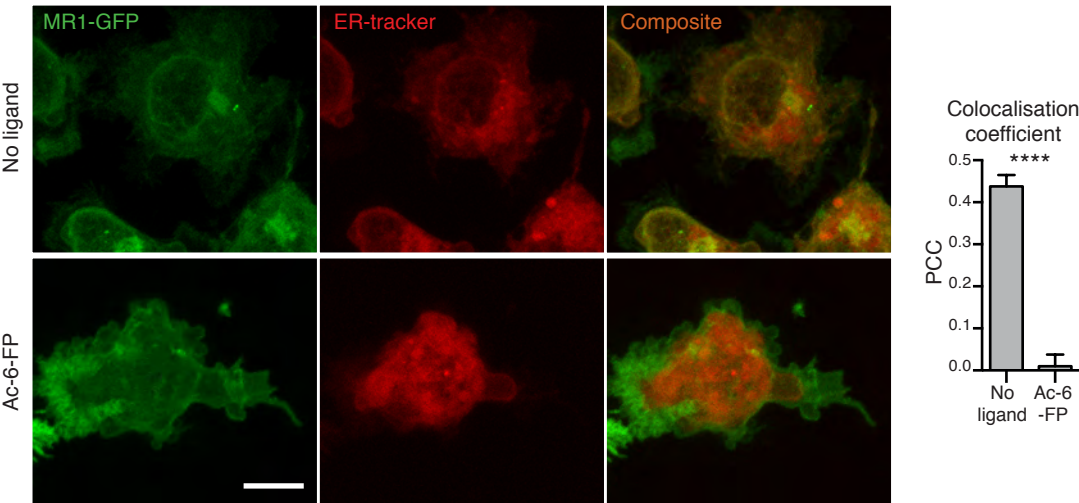
**a C1R.MR1 cells**



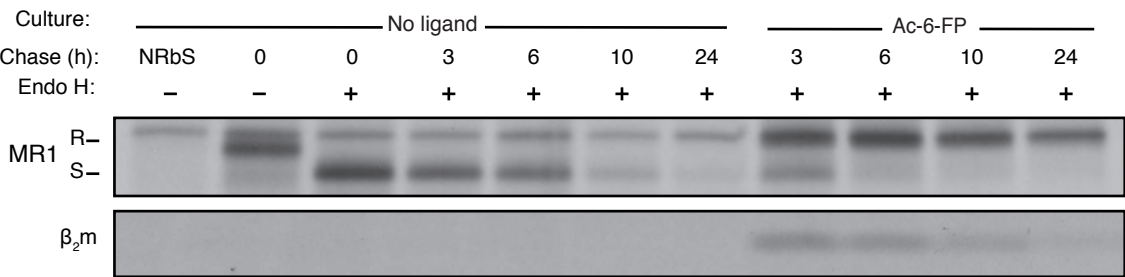
**b Peripheral blood mononuclear cells**



**c C1R.MR1-GFP cells**



**d <sup>35</sup>S radiolabelled C1R.MR1 cells**



**e <sup>35</sup>S radiolabelled C1R.MR1 cells**

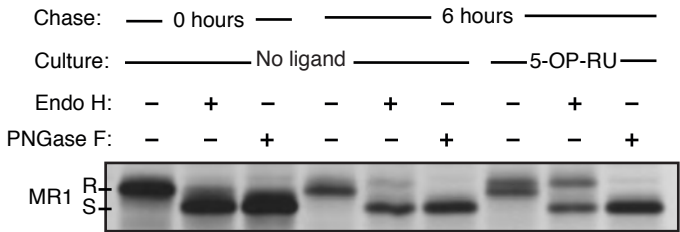
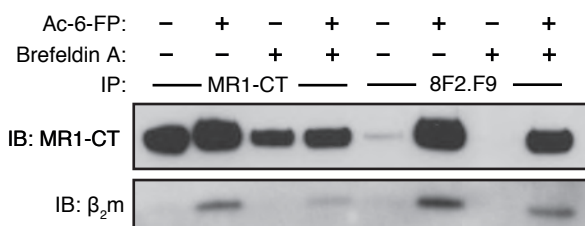
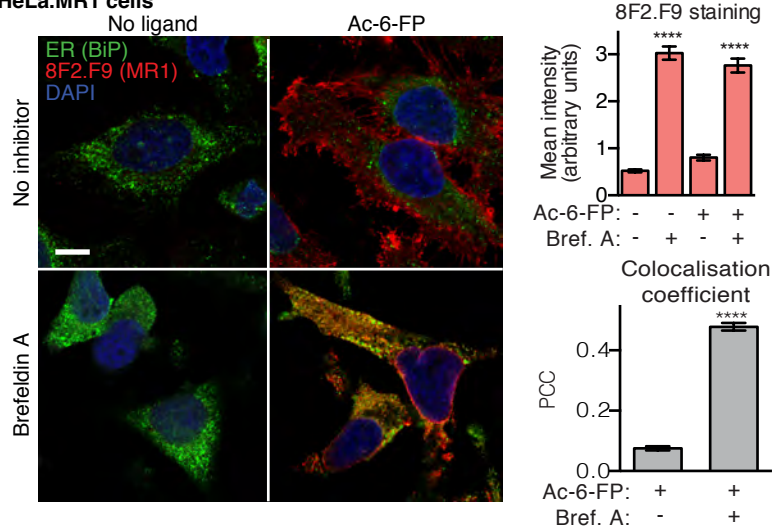


**Figure 4**

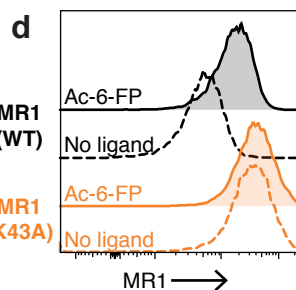
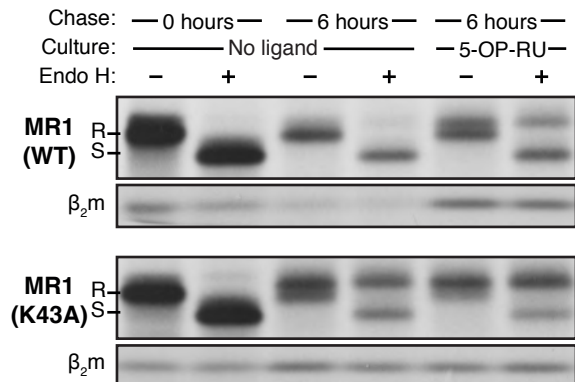
**a C1R.MR1 cells**



**b HeLa.MR1 cells**



**c  $^{35}S$  radiolabelled C1R.MR1 and C1R.MR1-K43A cells**



**e**

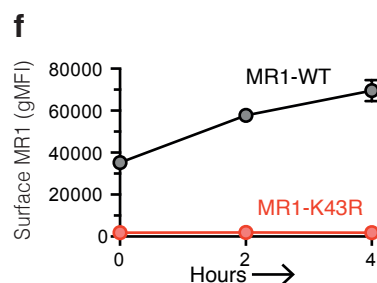
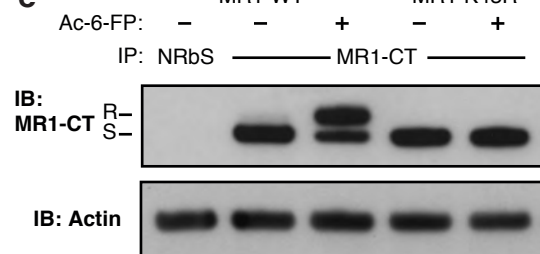
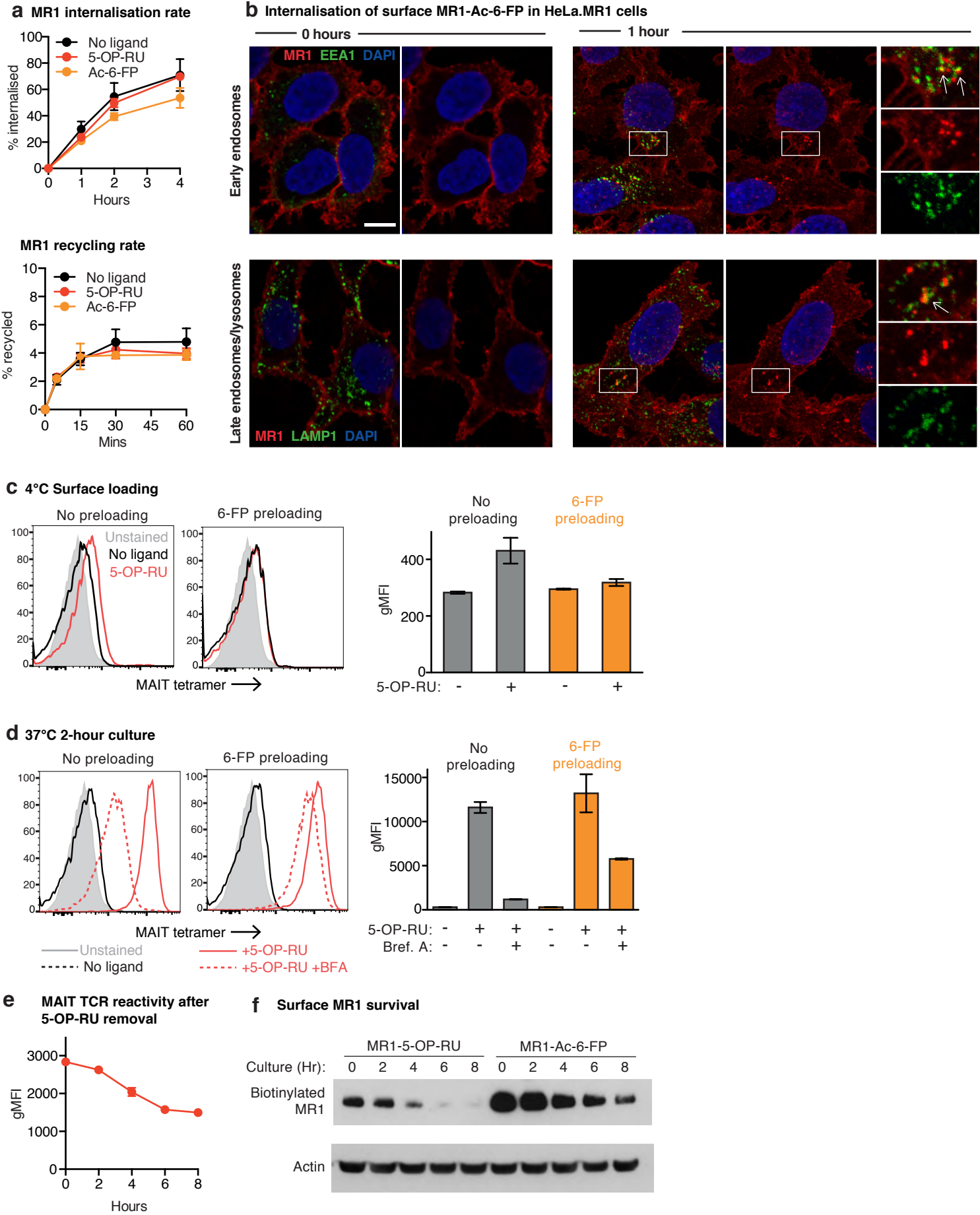
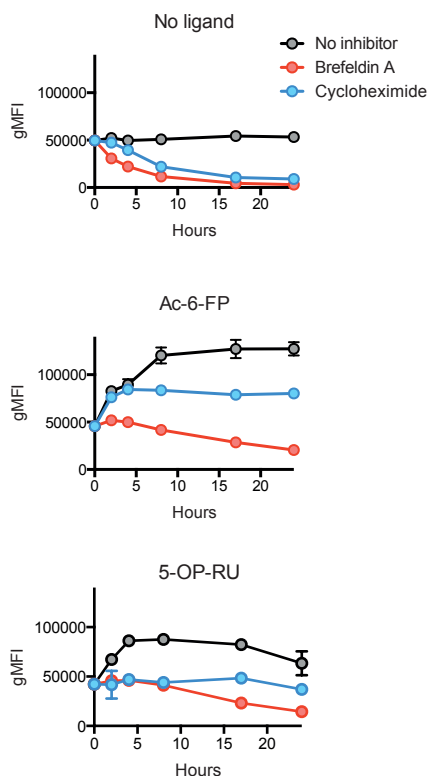


Figure 5

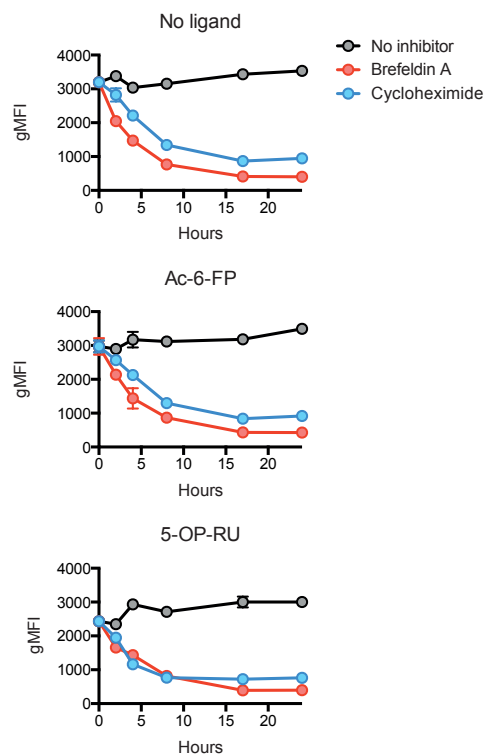


# Supplementary Figure 1: MR1 and MHC class I surface expression kinetics in C1R.MR1 cells

**a** MR1 surface expression kinetics

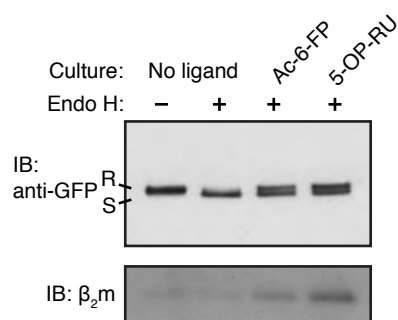


**b** MHC-I surface expression kinetics



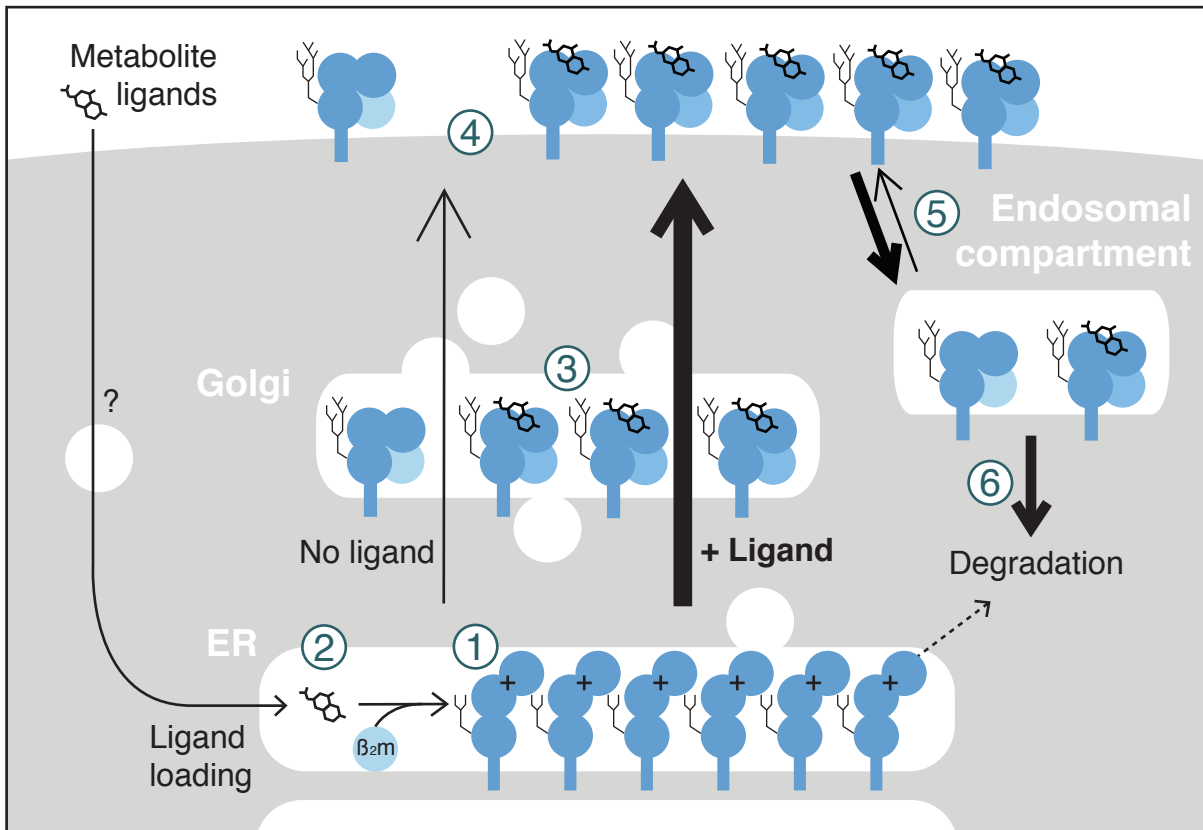
MR1 cell surface expression in C1R.MR1 cells (A) and MHC class I (MHC-I) expression in C1R and C1R.MR1 cells (B) measured by flow cytometry and represented as geometric mean fluorescence intensity (gMFI). Cells were incubated without ligands (upper graphs) or with 10  $\mu$ M Ac-6-FP (middle) or 5-OP-RU (lower). Surface expression is ablated by culturing with brefeldin A (red line) and less so with the protein synthesis inhibitor cycloheximide (blue line).

## Supplementary Figure 2: Ligands promote MR1-GFP maturation similarly to wild-type MR1



C1R cells transduced with MR1-GFP were cultured with or without 0.1 mM Ac-6-FP or 5-OP-RU for 6 hours. Cells were lysed and MR1-GFP was immunoprecipitated using anti-GFP agarose beads (GFP-Trap, Chromotek), and immunoblotted for GFP or  $\beta_2m$ . MR1-GFP is predominantly endo H susceptible in the absence of ligands, but becomes resistant with ligand culture.

**Supplementary Figure 3: MR1 trafficking schematic**



In the steady state, MR1 predominantly resides as an immature protein in the endoplasmic reticulum in an unfolded conformation (1). Ligands enter the cell via an unknown mechanism and load onto immature MR1 in the ER (2), where the charged lys43 (+) is neutralised and conformational folding occurs, including strong  $\beta_2m$  association. Traffic through the Golgi apparatus results in further glycosylation (3). Mature MR1 remains at the cell surface for several hours (4) and is internalised to the endosomal compartment (5), with a low level of recycling back to the surface. MR1 may be degraded from the endosomes or directly from the ER (6).